Editors' Suggestion | Featured in Physics

Noise-Induced Acceleration of Single Molecule Kinesin-1

Takayuki Ariga,[1,*] Keito Tateishi,[1] Michio Tomishige,[2] and Daisuke Mizuno[3]
[1]Graduate School of Medicine, Yamaguchi University, 755-8505 Yamaguchi, Japan
[2]Department of Physical Sciences, Aoyama Gakuin University, 252-5258 Kanagawa, Japan
[3]Department of Physics, Kyushu University, 819-0395 Fukuoka, Japan

(Received 16 March 2021; accepted 8 September 2021; published 22 October 2021)

The movement of single kinesin molecules was observed while applying noisy external forces that mimic intracellular active fluctuations. We found kinesin accelerates under noise, especially when a large hindering load is added. The behavior quantitatively conformed to a theoretical model that describes the kinesin movement with simple two-state reactions. The universality of the kinetic theory suggests that intracellular enzymes share a similar noise-induced acceleration mechanism, i.e., active fluctuations in cells are not just noise but are utilized to promote various physiological processes.

DOI: 10.1103/PhysRevLett.127.178101

Fluctuations are ubiquitous and prominent in microscopic systems. The effects of the fluctuations on motions and/or chemical reactions are a long-studied field of nonequilibrium physics [1–8], and their relevance in biological systems is emerging as a hot topic [9–18]. Recently, direct observations *in vitro* have confirmed that motor proteins are violently shaken by thermal fluctuations [19]. The walking molecular motor, kinesin-1 (hereafter called kinesin), which carries vesicles on microtubules in cells [20], has long been proposed to utilize thermal fluctuations to make directed movements [3]. In addition to thermal fluctuations, living cells actively generate nonthermal fluctuations using energy derived from metabolic activities [10–12]. However, it is not clear whether and how these active fluctuations affect the function of kinesins in living cells.

In our previous study, we investigated the energetics of single-molecule kinesin *in vitro* [21], where the energy input-output balance of working kinesin was obtained using a novel nonequilibrium equation, the Harada-Sasa equality [22]. Whereas ∼50% efficiency of kinesin has been reported at stall-force conditions [23], we observed only 20% power efficiency at working conditions and found that ∼80% of the input free energy obtained from adenosine triphosphate hydrolysis ($\Delta\mu$) was not transmitted to cargo movement but dissipated via hidden paths [21], implying that kinesin has low efficiency [24]. However, it is hard to imagine that kinesin, which has been preserved after billions of years of molecular evolution, would be inefficient at cargo transport. Therefore, we hypothesized that kinesin is optimized for its actual working environment, *living cells*, but not necessarily *in vitro* [25]. The effects of these active fluctuations, which do not exist in experimental conditions *in vitro* but do occur in living cells [10–12], on the functions of individual motors are unknown.

In this study, to investigate the effects of active fluctuations on single kinesin molecules, we used an *in vitro* measurement system to apply actively fluctuating external forces (i.e., noise), artificially mimicking intracellular active fluctuations [Fig. 1(a)]. The results show that kinesin accelerates in response to the applied noise, especially under the application of a large average hindering force (load), indicating that kinesin is optimized to its actively fluctuated working environment. Moreover, the acceleration was quantitatively explained with a mathematical model using independently determined parameters. Because of the universality of the theories behind the model, the noise-induced acceleration found in kinesin is widely applicable to other general enzymes in cells.

Active fluctuations within eukaryotic cells are mostly derived from actomyosins in cytoskeletal networks [9,11]. It has been reported that the distribution of myosin-generated fluctuations is heavily tailed in a manner similar to a Lévy stable distribution rather than a simple Gaussian distribution [13]. To reproduce the intracellular active fluctuations *in vitro*, we numerically generated Lévy-like stochastically fluctuating signals [26] and applied these signals as external forces via an optical trap to a probe bead that acted as a cargo carried by kinesin [Fig. 1(a), see Methods in the Supplemental Material [27]]. The position of the laser focus was controlled within 100 ± 100 nm from the bead center due to the technical limitation of the optical tweezers. The applied noise was therefore truncated by replacing values above the limit with an upper (or lower) limit, which we term "semitruncated Lévy noise" [Fig. 2(a)]. Note that Lévy noise cannot be realized in physical systems in its exact mathematical form. Rather, semitruncated Lévy noise more resembles the non-Gaussian fluctuations that have been found in various physical systems far from equilibrium, including active swimmer suspensions [14–16], actomyosin networks [13], and cultured cells [17].

Semitruncated Lévy noise was applied to a single kinesin molecule in addition to a constant force (load) [Fig. 2(b)].

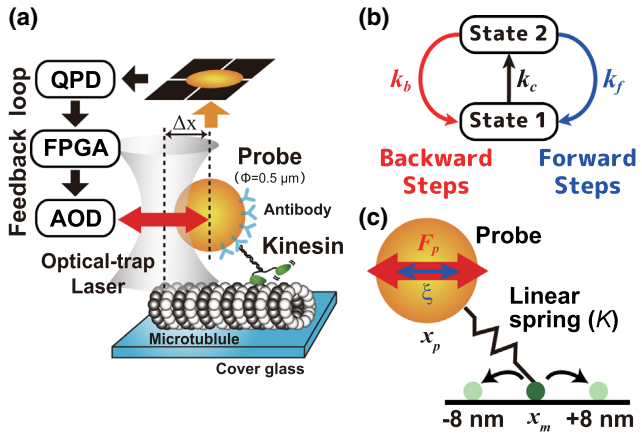

FIG. 1. (a) Schematic of the measurement system (not to scale). A single kinesin molecule is attached to an ~500 nm diameter probe particle via anti-His-tag antibody. The probe is trapped with a focused infrared laser (optical tweezers) and directed to the microtubule rail to detect kinesin movement. The probe position is obtained by projecting the image to the quadrant photodiode detector (QPD) using bright field illumination. The output voltage signal is acquired by the field programmable gate array (FPGA) board to calculate the trap position. The trap position is controlled by the output signal from the FPGA board via acousto-optic deflectors (AOD). By changing the distance between the trap and probe position (Δx: trap distance) through programming of the FPGA, an arbitrary external force, $F_p = k_{\text{trap}}\Delta x$, where k_{trap} is trap stiffness, can be applied to the probe particle at an update rate of 20 kHz, which is the same as the sampling rate. Here, we applied external forces to the probe as $F_p = F_0 + F_n$, where F_0 is a constant force (load) and F_n is a zero-mean fluctuating force (noise). (b) The two-state mathematical model for kinesin. Transitions between two internal states contain load-independent (k_c) and load-dependent (k_f and k_b) transitions. k_f and k_b have an Arrhenius-type force dependency [Eq. (1)] that are coupled to forward and backward steps, respectively. (c) The Langevin model of the probe movement that is pulled by the kinesin molecule. The kinesin molecule is modeled as a jumping point with 8-nm back and forth steps (x_m), while the probe (x_p) is connected to the kinesin via a linear spring. The external force F_p, including an average load F_0, and a zero-mean fluctuating force F_n, is applied to the probe, which is exposed to a thermal fluctuating force ξ.

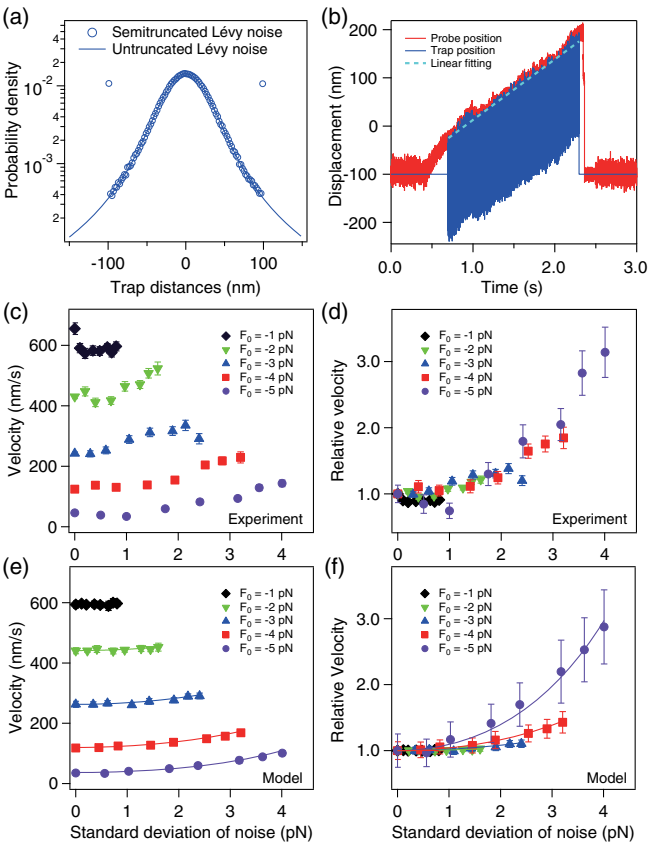

FIG. 2. (a) Distribution of semitruncated Lévy noise. *Circles* indicate the distribution of the trap distance used in the experiments and simulations (scale parameter $\gamma = 20$ nm; see Eq. (S3) in the Supplemental Material [27]), where trap distances over ± 100 nm are truncated to ± 100 nm. *Line* indicates the corresponding untruncated Lévy distribution calculated by numerical integration with Eq. (S2) in Ref. [27]. (b) A typical trajectory of a probe particle pulled by a single kinesin molecule under semitruncated Lévy noise. The external force is applied as $F_0 = -4$ pN constant force (load) by keeping the trap distance 100 nm at a trap stiffness of 0.04 pN/nm along with a mean-zero fluctuating force (noise) F_n, with scale parameter $\gamma = 20$ nm, which truncated the trap distance to ± 100 nm. *Dotted line* indicates linear fitting of the probe trajectory to obtain the average velocity. (c) The velocity of the probe particles under semitruncated Lévy noise of various magnitudes [mean $\pm$ standard error (s.e.); $n = 44$ to 134]. Each *marker* indicates different average loads ($F_0 = -1$ to -5 pN). The horizontal axis is normalized to the standard deviation (s.d.) of the noise, $\langle F_n^2 \rangle^{1/2}$. (d) Relative velocities of the probe using the same conditions as (c). The relative velocities were calculated as the velocity divided by the velocity without noise at the same load. (e) Numerical simulations for the velocity of the probe under semitruncated Lévy noise of various magnitudes (*marker*, mean $\pm$ s.d.; $n = 10$). (f) Relative velocities of the data in (e). *Solid lines* indicate theoretical predictions from Eqs. (S5) and (S8) in Ref. [27]; see also Appendix B.

The average velocities and relative velocities, which are the ratio of the average velocity with and without added noise, are shown in Figs. 2(c) and 2(d). Each *marker* indicates the average load ($-1 \sim -5$ pN), and the horizontal axis is normalized by the standard deviation (s.d.) of the fluctuations (noise) of the applied force. At each average load, the motor velocity gradually increased with the magnitude of the noise. The larger the load, the larger the increase in relative velocity due to the noise, but a smaller change was observed at low loads.

To examine the observed accelerating behavior of kinesin, we performed numerical simulations with our previously reported mathematical model [21]. The kinesin movement was modeled by the simplified kinetic model with two internal states that are connected by force-independent (k_c) and -dependent (k_f and k_b) transitions [37] [Fig. 1(b)]. k_f and k_b have an Arrhenius-type force dependency [23]:

$$k_{\{f,b\}}(F_m) = k^0_{\{f,b\}} \exp\left(\frac{d_{\{f,b\}} F_m}{k_B T}\right), \quad (1)$$

where $k^0_{\{f,b\}}$ is the rate constant at zero force, $d_{\{f,b\}}$ is the characteristic distance, k_B is the Boltzmann constant, T is the absolute temperature, and F_m is the force applied to the motor. The subscripts f and b indicate forward and backward 8-nm steps, respectively. The simulations were conducted with Langevin dynamics of the probe, which is connected to the kinetic kinesin model via an elastic linker [Fig. 1(c)], using

$$\Gamma \frac{d}{dt} x_p = K(x_m - x_p) + F_p + \xi, \quad (2)$$

where Γ is the viscous drag, K is the spring constant of the stalk, and x_p and x_m are the position of the probe and motor, respectively. The external force to the probe, $F_p = F_n + F_0$, contains a constant force (load) F_0, and a fluctuating force (noise) F_n, with zero mean, and ξ is white Gaussian thermal fluctuations that satisfy $\langle \xi \rangle = 0$ and $\langle \xi(t)\xi(t') \rangle = 2k_B T \Gamma \delta(t - t')$, where $\delta(t)$ is the delta function. Note that although kinesin has a nonlinear spring and we have confirmed that the spring constant depends on the external force (Fig. S2b in Ref. [27]), the numerical simulations were performed with a constant K for each average load F_0, with K measured at each constant load (F_0). Remarkably, despite all parameters being experimentally determined without noise (See Figs. S1, S2 and Appendix A in the Supplemental Material [27]), the simulations under semitruncated Lévy noise [Figs. 2(e) and 2(f), *markers*] show fairly similar output to the experimental conditions with noise [Fig. 2(c) and 2(d)].

Although the noise amplitudes in the above measurements are experimentally limited, simulations can be conducted at conditions exceeding the constraints. In realistic intracellular conditions, the metabolic activity of actomyosins is expected to generate much larger noise [11], where the maximum force derived from the myosin minifilament is estimated to be over 30 pN [38]. Therefore, we conducted simulations in which the noise distribution was truncated at a physiologically plausible value of 30 pN [Fig. 3(a)], indicating that the velocity at the unloaded, noiseless condition could be achieved regardless of the average load. Since the average load can be regarded as the resistance to high viscosity in cells [39], kinesin is thought to optimally utilize active fluctuations to achieve the same velocity as unloaded conditions in low viscous solutions.

The noise-induced acceleration observed here can be qualitatively explained by Jensen's inequality:

$$\langle k(F) \rangle \geq k(\langle F \rangle), \quad (3)$$

where $< >$ indicates average, and k is a convex function of F. Here, we regard k as the kinetic rate and F as the applied

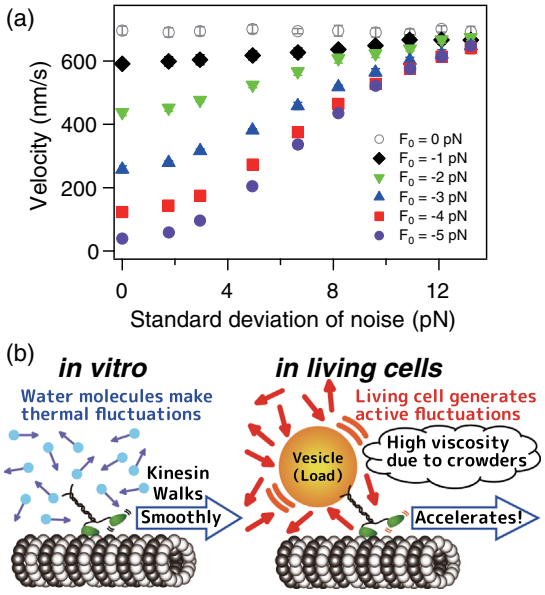

FIG. 3. (a) Numerical simulations for the velocities of the probe under semitruncated Lévy noise limited to ±30 pN (i.e., physiological forces that exist in living cells [38]; mean ± s.d.; $n = 10$). (b) Schematic drawing of the physiological implications of the noise-induced acceleration of kinesin. Kinesin utilizes thermal fluctuations to walk smoothly *in vitro* (*left*). When kinesin carries a vesicle within a living cell, it is expected that the kinesin utilizes the non-thermal fluctuations actively produced by the cell to achieve the same velocity as at no load even when intracellular crowders generate high viscosity (*right*).

external force that contains both constant and fluctuating forces. As presented in Eq. (1), $k(F)$ is expressed by the Arrhenius equation, i.e., an exponential function [23]. In this case, Jensen's inequality tells us that the average of the rate constants generally increases when F fluctuates. The universality of Jensen's inequality and the Arrhenius equation implies that any enzyme obeying the same Arrhenius equation can experience noise-induced acceleration.

The results so far show the effect of *white* noise applied to the probe. It is known, however, that actual intracellular fluctuations have a large frequency dependency [11,12]. To investigate the frequency dependency of the kinesin acceleration, we applied sinusoidal noise oscillating at different frequencies with a larger amplitude than the linear response range [21] and measured the average velocity. The acceleration showed a characteristic dependency on the frequency that peaked at ~200 Hz [Fig. 4(a)]. This tendency was also reproduced by numerical simulations [Fig. 4(b)]. These results indicate that the noise-induced acceleration strongly depends on its frequency characteristics.

Kinesin transports sub-μm sized vesicles or larger organelles within cells. In this study, instead of cargoes, force fluctuations were applied to the probe particle and indirectly transmitted to kinesin via the elastic linker. Thus, rapid fluctuations were attenuated due to the slow response of the probe. This attenuation can be explained by the Langevin

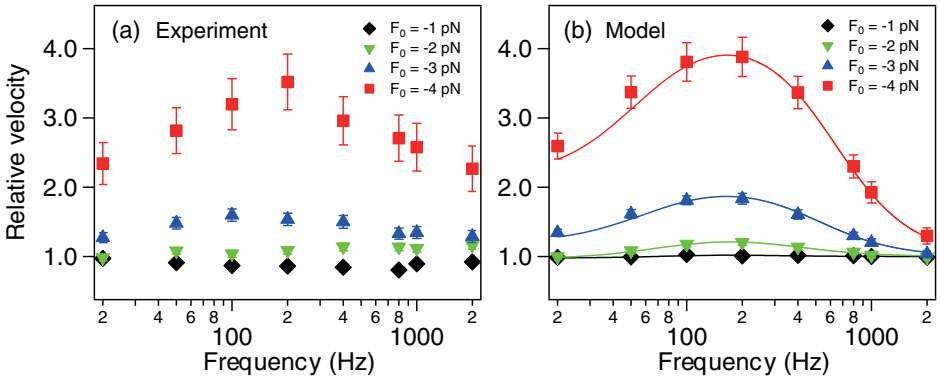

FIG. 4. (a) The relative velocities of the probe particles under sinusoidal noise of various frequencies (mean ± s.e; $n = 39$ to 173). An external force, $F_p = F_0 + A\sin(ft)$, was applied as a constant force (load), F_0, plus zero-mean sinusoidal forces with an amplitude of A, where the amplitude of the sinusoidal noise is the same as the load ($A = F_0$) at different frequencies, f. Different *markers* indicate different average loads ($F_0 = 0$ to -4 pN). (b) Numerical simulations for the relative velocities of the probe particles under sinusoidal noise of various frequencies (*markers*, mean ± s.d.; $n = 10$). *Solid lines* indicate the theoretical predictions from Eq. (S13) in Methods in the Supplemental Material [27]; see also Appendix C.

model of the probe [Fig. 1(c) and Appendix B in the Supplemental Material [27]]. Simulations of the acceleration applying a simple Gaussian noise did not fit well with the theoretical prediction from the kinetic kinesin model but did agree with the prediction considering the response of the probe (Fig. S3 in Ref. [27]). Surprisingly, the theoretical prediction with simple Gaussian noise can quantitatively explain the simulations that applied semitruncated Lévy noise [Fig. 2, *solid lines*, Eqs. (S5) and (S8) in the Supplemental Material [27]] without parameter modifications. In addition, we performed the velocity measurements by applying semitruncated Gaussian noise, which was also quantitatively explained by the same prediction (Fig. S4 in Ref. [27]). These results suggest that the acceleration of kinesin is mainly determined by the magnitude (s.d.) of the applied noise, but it is insensitive to the shape of the noise distribution, at least under our experimental conditions.

The acceleration under sinusoidal noise tended to decrease even at lower frequencies (Fig. 4), where the probe fluctuation is sufficiently transmitted to kinesin. The attenuation at low frequencies can be explained based on the kinetic model of kinesin [Fig. 1(b), Appendix C in Ref. [27]]. The perturbation expansion of the theory predicts that the acceleration has a similar characteristic frequency to the linear response as kinesin movements to the applied external force [21]. By estimating the high- and low-frequency limits of kinesin velocity, we quantitatively explained the frequency dependency of the kinetic kinesin model (Fig. S5 in the Supplemental Material [27]). Taken together, the ∼200 Hz peak of the observed acceleration was quantitatively explained [Fig. 4(b), *lines*].

In our experiments, external forces were applied only to the direction of pulling backward; no force was applied in the forward direction due to the experimental limitations (Methods in Ref. [27]). The simulations applying noises without the limitations revealed that no remarkable acceleration was observed under the condition at which the average load is zero [Fig. 3(a) and Fig. S6 in the Supplemental Material [27], *open circles*]. In contrast, it was observed that another microtubule-based motor, dynein, moves faster when experiencing an external force shaking back and forth [18]. However, simulations with the same situation indicated that kinesin slows down in response to low-frequency rectangular pulse oscillations (Fig. S7 in Ref. [27]). The contrasting behaviors of the two motor proteins can be explained by the same mechanism, i.e., averaging the force-velocity relationship at forward and backward constant loads [18,27], indicating that the acceleration due to the slow back-and-forth oscillation is not a universal property but only occurs with a concave shape force-velocity relationship. On the other hand, in this Letter, the acceleration of kinesin was observed under physiologically plausible fluctuations, where the total force was always applied backward and never directly forward. The different behaviors suggest that the noise-induced acceleration found in kinesin has a distinct mechanism from that previously found in dynein [18]. Because intracellular kinesins transporting cargoes are always enduring viscous drag, our application of noise in addition to the hindering load could better represent kinesins in the working environment.

Although its acceleration response due to the low-frequency oscillation depends on the shape of the F-V relationship, dynein can also be expected to perform the same acceleration phenomenon observed in kinesin if active fluctuations are applied in the same relatively high-frequency range as used here and in intracellular conditions. Regardless of the details of the mathematical model, i.e., the shape of the graph combining each transition process, which depends on the kinetic scheme of the motor and generally differs between molecular motors, the external force dependence of each transition

process is predicted to behave with common Arrhenius-type force dependency [Eq. (1) and as used in Ref. [18]]. Therefore, the acceleration due to Jensen's inequality can always be predicted. Moreover, not only these molecular motors, but general enzymes also act with structural changes and obey the same Arrhenius equation. Thus, the noise-induced acceleration found in kinesin can be extrapolated to any molecular machine working in living cells.

So far, we have investigated only the steady-state properties, where kinesins are always moving along microtubules processively. Actual kinesin, however, stochastically dissociates from the microtubules after ∼100 steps [40]. This dissociation becomes significantly faster when pulled forward than when pulled backward [41]. Thus, the addition of external forces in the forward direction (assisting force) makes the kinesin-tethered cargo dissociate rapidly from the microtubules. This property found in kinesin is completely different from full-length dynein dimers, which accelerate in response to the assisting force, but resembles the behavior of monomeric dynein [18]. Unlike Feynman's ratchet-type dynein, kinesin may save energy by rapidly dissociating from the microtubule in response to assisting forces, where the cargo is likely to be passively carried by the intracellular active fluctuations.

In an actual living cell, the high viscosity is realized by molecular crowding [42,43]. Thus, the result in Fig. 3(a) indicates that the unloaded velocity measured at low viscosity can be achieved by using active fluctuations even under crowding conditions [Fig. 3(b)]. However, intracellular crowders affect not only the movement of cargo through the viscosity but also the diffusion of kinesin's individual motor domains [44], meaning that the presence of crowders *per se* changes the motor's activity. Moreover, whereas the crowding state within cells is dense enough to freeze the dynamics due to a glass transition, a living cell's finite viscosity is achieved by fluidizing through active fluctuations [45]. Therefore, only considering the effect of high viscosity is insufficient to discuss motor activity within cells. Thus, the next challenge is to develop *in vitro* conditions that mimic the intracellular crowding environment with abundant crowders that have active fluctuations.

In summary, we show that an active fluctuating force accelerates the movement of single kinesin molecules, especially under high loads, suggesting that kinesin can move fast even under intracellular crowding conditions. Because the active fluctuations in cells are generated by the metabolic activity of a large number of motor molecules, the fluctuations *per se* consume large energies. Thus, the efficiency of each accelerated kinesin is apparently very low. Instead of the efficiency, as mentioned at the beginning of this Letter, a different quantitative measure of the optimization, or fitness, for their working environment is desired. In addition, the acceleration is quantitatively explained by two universal theories, Jensen's inequality and the Arrhenius equation. Because general enzymes obey the same Arrhenius equation, intracellular active fluctuations should not be thought as just noise but as a sort of "vitality of life" that improves molecular activities in general.

One unresolved problem is that the velocities of vesicles transported by kinesin in cells are much faster than those observed *in vitro* [46]. Other factors have been implicated in vesicle transport within living cells, and some have been indicated to accelerate kinesin movement [47]. Our bottom-up approach, which approximates the *in vitro* assay to the intracellular active environment and gives an analysis that utilizes universal theories, sheds light on the physical or physiological principles underlying the use of active fluctuations by general biomolecules.

We thank Professor Mutsunori Shirai and Professor Makoto Furutani-Seiki for their kind permission for us to conduct our own research; Professor Sin-ichi Sasa, Professor Masahiro Ueda, and Professor Shuji Ishihara for valuable discussions; and Dr. Peter Karagiannis for critically revising the manuscript. This work was supported by JSPS KAKENHI (JP15K05248, JP18K03564, JP19H05398, JP20H05535, and 21H00405 to T. A. and JP20H05536 and JP25103011 to D. M.).

*ariga@yamaguchi-u.ac.jp

[1] F. Oosawa, J. Theor. Biol. **52**, 175 (1975).
[2] R. D. Astumian, P. B. Chock, T. Y. Tsong, Y. D. Chen, and H. V. Westerhoff, Proc. Natl. Acad. Sci. U.S.A. **84**, 434 (1987).
[3] R. D. Vale and F. Oosawa, Adv. Biophys. **26**, 97 (1990).
[4] N. J. Cordova, B. Ermentrout, and G. F. Oster, Proc. Natl. Acad. Sci. U.S.A. **89**, 339 (1992).
[5] M. O. Magnasco, Phys. Rev. Lett. **71**, 1477 (1993).
[6] R. D. Astumian and M. Bier, Phys. Rev. Lett. **72**, 1766 (1994).
[7] J. Prost, J.-F. Chauwin, L. Peliti, and A. Ajdari, Phys. Rev. Lett. **72**, 2652 (1994).
[8] C. R. Doering, W. Horsthemke, and J. Riordan, Phys. Rev. Lett. **72**, 2984 (1994).
[9] D. Mizuno, C. Tardin, C. F. Schmidt, and F. C. MacKintosh, Science **315**, 370 (2007).
[10] Bradley R. Parry, Ivan V. Surovtsev, Matthew T. Cabeen, Corey S. O'Hern, Eric R. Dufresne, and C. Jacobs-Wagner, Cell **156**, 183 (2014).
[11] M. Guo, Allen J. Ehrlicher, Mikkel H. Jensen, M. Renz, Jeffrey R. Moore, Robert D. Goldman, J. Lippincott-Schwartz, Frederick C. Mackintosh, and David A. Weitz, Cell **158**, 822 (2014).
[12] K. Nishizawa, M. Bremerich, H. Ayade, C. F. Schmidt, T. Ariga, and D. Mizuno, Sci. Adv. **3**, e1700318 (2017).
[13] I. Zaid, H. L. Ayade, and D. Mizuno, Biophys. J. **106**, 171a (2014).
[14] I. Zaid and D. Mizuno, Phys. Rev. Lett. **117**, 030602 (2016).
[15] T. Kurihara, M. Aridome, H. Ayade, I. Zaid, and D. Mizuno, Phys. Rev. E **95**, 030601(R) (2017).

[16] K. Kanazawa, T. G. Sano, A. Cairoli, and A. Baule, Nature (London) **579**, 364 (2020).
[17] É. Fodor, M. Guo, N. S. Gov, P. Visco, D. A. Weitz, and F. van Wijland, Europhys. Lett. **110**, 48005 (2015).
[18] Y. Ezber, V. Belyy, S. Can, and A. Yildiz, Nat. Phys. **16**, 312 (2020).
[19] H. Isojima, R. Iino, Y. Niitani, H. Noji, and M. Tomishige, Nat. Chem. Biol. **12**, 290 (2016).
[20] R. D. Vale, Cell **112**, 467 (2003).
[21] T. Ariga, M. Tomishige, and D. Mizuno, Phys. Rev. Lett. **121**, 218101 (2018).
[22] T. Harada and S.-i. Sasa, Phys. Rev. Lett. **95**, 130602 (2005).
[23] J. Howard, *Mechanics of Motor Proteins and the Cytoskeleton* (Sinauer Associates, Inc., Sunderland, 2001).
[24] A. G. Hendricks, Physics **11**, 120 (2018).
[25] T. Ariga, M. Tomishige, and D. Mizuno, Biophys. Rev. **12**, 503 (2020).
[26] J. M. Chambers, C. L. Mallows, and B. Stuck, J. Am. Stat. Assoc. **71**, 340 (1976).
[27] See Supplemental Material at http://link.aps.org/supplemental/10.1103/PhysRevLett.127.178101 for the detailed methods, the derivations for theoretical lines, and Supplemental Figures S1–S7, which includes Refs. [28–36].
[28] T. Aoki, M. Tomishige, and T. Ariga, Biophysics **9**, 149 (2013).
[29] T. Mori, R. D. Vale, and M. Tomishige, Nature (London) **450**, 750 (2007).
[30] M. J. Lang, C. L. Asbury, J. W. Shaevitz, and S. M. Block, Biophys. J. **83**, 491 (2002).
[31] S. Chandrasekhar, Rev. Mod. Phys. **15**, 1 (1943).
[32] F. Gittes and C. F. Schmidt, Methods Cell Biol. **55**, 129 (1997).
[33] C. Hyeon, S. Klumpp, and J. N. Onuchic, Phys. Chem. Chem. Phys. **11**, 4899 (2009).
[34] B. E. Clancy, W. M. Behnke-Parks, J. O. Andreasson, S. S. Rosenfeld, and S. M. Block, Nat. Struct. Mol. Biol. **18**, 1020 (2011).
[35] M. Nishiyama, H. Higuchi, and T. Yanagida, Nat. Cell Biol. **4**, 790 (2002).
[36] N. J. Carter and R. A. Cross, Nature (London) **435**, 308 (2005).
[37] Y. Taniguchi, M. Nishiyama, Y. Ishii, and T. Yanagida, Nat. Chem. Biol. **1**, 342 (2005).
[38] M. Kaya, Y. Tani, T. Washio, T. Hisada, and H. Higuchi, Nat. Commun. **8**, 16036 (2017).
[39] D. Wirtz, Annu. Rev. Biophys. **38**, 301 (2009).
[40] R. D. Vale, T. Funatsu, D. W. Pierce, L. Romberg, Y. Harada, and T. Yanagida, Nature (London) **380**, 451 (1996).
[41] B. Milic, J. O. Andreasson, W. O. Hancock, and S. M. Block, Proc. Natl. Acad. Sci. U.S.A. **111**, 14136 (2014).
[42] R. J. Ellis, Trends Biochem. Sci. **26**, 597 (2001).
[43] D. S. Goodsell, Trends Biochem. Sci. **16**, 203 (1991).
[44] K. Sozański, F. Ruhnow, A. Wiśniewska, M. Tabaka, S. Diez, and R. Hołyst, Phys. Rev. Lett. **115**, 218102 (2015).
[45] K. Nishizawa, K. Fujiwara, M. Ikenaga, N. Nakajo, M. Yanagisawa, and D. Mizuno, Sci. Rep. **7**, 15143 (2017).
[46] J. L. Ross, Biophys. J. **111**, 909 (2016).
[47] K. Chiba *et al.*, Mol. Biol. Cell **25**, 3569 (2014).